Available online at www.sciencedirect.com
SCIENCE DIRECT®

Journal of the European Ceramic Society 23 (2003) 2163–2169
www.elsevier.com/locate/jeurceramsoc

Fabrication of textured bismuth titanate by templated grain growth using aqueous tape casting

Yanmei Kan[a], Peiling Wang[a,*], Yongxiang Li[a], Yi-Bing Cheng[b], Dongsheng Yan[a]

[a]*The State Key Lab of High Performance Ceramics and Superfine Microstructure, Shanghai Institute of Ceramics, Chinese Academy of Sciences, Shanghai 200050, China*

[b]*School of Physics and Materials Engineering, Monash University, Clayton, Victoria, 3800, Australia*

Received 11 September 2002; received in revised form 27 December 2002; accepted 13 January 2003

Abstract

Textured bismuth titanate ($Bi_4Ti_3O_{12}$) ceramics were fabricated by templated grain growth (TGG), using plate-like $Bi_4Ti_3O_{12}$ particles prepared by a molten salt method as the templates. The templates were aligned in the fine-grained matrix by aqueous tape casting with their major surface parallel to the casting plane. Effect of sintering conditions on the grain orientation in the material was investigated. It was found that the degree of grain orientation (Lotgering factor, f) increased with the increase in sintering temperature, soaking time and heating rate. High Lotgering factor ($f \geqslant 0.92$) can be obtained through careful control of the sintering parameters. The textured $Bi_4Ti_3O_{12}$ ceramics showed a high anisotropy in its dielectric properties in the directions parallel and perpendicular to the casting plane.

Keywords: Aqueous tape casting; $Bi_4Ti_3O_{12}$; Dielectric properties; Grain growth; Microstructure-final; Platelets

1. Introduction

Texture structured ceramics have attracted increasing attention, because of their improved electrical, mechanical and other properties.[1–3] Although textured ceramics can be produced by hot forming techniques,[1,4–6] the high cost of these methods makes it unsuitable for commercial production. Templated grain growth (TGG) is a cost effective technique for mass production of textured ceramics. In this method, the textured microstructure is obtained via grain growth of anisometric template particles aligning in a fine-grained matrix. Up to now, a variety of materials, such as Si_4N_3, Al_2O_3, SiC, $Sr_{0.53}Ba_{0.47}Nb_2O_6$ and $Bi_4Ti_3O_{12}$,[2,7–10] have been fabricated by TGG, and enhanced properties are achieved from these materials.

Bismuth titanate ($Bi_4Ti_3O_{12}$) is a well-known family member of the layer-structured bismuth compound. It shows a high Curie temperature of 675 °C,[11] and is a good candidate for high temperature applications. However, there is difficulty in poling $Bi_4Ti_3O_{12}$ ceramics, because the layered structure and low crystal symmetry of $Bi_4Ti_3O_{12}$ inhibit appropriate orientation of the polarization axes. Fabrication of textured microstructures stands for an effective means to improve the performance of $Bi_4Ti_3O_{12}$.

Previous works on preparing textured $Bi_4Ti_3O_{12}$ ceramics by TGG often used organic solutions to prepare slurries for tape casting.[10] The organic solutions used were expensive and sometimes even toxic and harmful to the environment and human health. Aqueous tape casting shows many advantages over organic tape casting in lowering the production costs and environment protection, although it is generally more difficult to prepare aqueous slurries suitable for tape casting than to prepare non-aqueous slurries. To our knowledge, no report on the fabrication of $Bi_4Ti_3O_{12}$ by aqueous tape casting has been made in the existing literature.

In the present study, textured $Bi_4Ti_3O_{12}$ was produced by TGG in combination with aqueous tape casting. The effect of sintering conditions on the grain orientation of the materials and the dielectric properties of the textured $Bi_4Ti_3O_{12}$ were investigated.

* Corresponding author. Tel.: +86-21-5241-2324; fax: +86-21-5241-3122.
E-mail address: plwang@sunm.shcnc.ac.cn (P. Wang).

0955-2219/03/$ - see front matter © 2003 Elsevier Science Ltd. All rights reserved.
doi:10.1016/S0955-2219(03)00035-9

2. Experimental

2.1. Preparation of $Bi_4Ti_3O_{12}$ templates

$Bi_4Ti_3O_{12}$ powder of stoichiometric composition was prepared by a hydrolysis method described in a previous paper.[12] This powder showed a BET surface area of 6.7 m^2/g and an average particle size of 0.2 μm. $Bi_4Ti_3O_{12}$ template particles were prepared by a molten-salt method. Equal weight of amorphous $Bi_4Ti_3O_{12}$ powder and Na_2SO_4/K_2SO_4 eutectic mixture were mixed in a sealed alumina crucible and heated at 1000 °C for 0.5 h. After slowly cooling to the room temperature, the reaction product was washed with hot de-ionized water to remove the sulfate salts, and then dried at 90 °C. The $Bi_4Ti_3O_{12}$ particles obtained were plate-like with a diameter of 3–4 μm and a thickness of 0.3 μm. TEM observation showed that they were single crystals with the *c*-axis perpendicular to their major surface planes.

2.2. Slurry preparation and tape casting

For slurry preparation, 20 vol.% $Bi_4Ti_3O_{12}$ powder was dispersed in de-ionized water using 0.5 wt.% (on the dry weight basis) commercial acrylic acid/acrylic ester copolymer as a dispersant (Acumer 2000, Rohm and Haas, USA), and the pH value was adjusted to pH 9 with analytical grade ammonia. The slurry was ball-milled for 48 h. In the middle of the ball milling, 5 wt.% (on the dry weight basis) polyvinyl alcohol (PVA) and 2.5 wt.% (on the dry weight basis) glycerin were added as a binder and a plasticizer, respectively.

$Bi_4Ti_3O_{12}$ platelets (5 wt.% of the fine powder) were dispersed in de-ionized water beforehand under continuous sonicating with the copolymer as dispersant. After completion of the ball milling process for the $Bi_4Ti_3O_{12}$ slurry, the $Bi_4Ti_3O_{12}$ platelets were mixed with the $Bi_4Ti_3O_{12}$ slurry under electromagnetic stirring for 16 h. Finally, the slurry was degassed under vacuum and tape cast on a glass surface at a speed of 6.0 cm/s and a blade opening of 120 μm. The tapes obtained were dried at room temperature, cut into pieces of 6×10 mm^2 and stacked at a pressure of 80 MPa for 10 min. The binder and plasticizer were burned out at a temperature of 600 °C for 3 h with a heating rate of 1 °C/min. To avoid the volatilization of bismuth during sintering, the laminates were buried in a $Bi_4Ti_3O_{12}$ packing powder with 0.5 wt.% excessive Bi_2O_3 and sealed in an alumina crucible, then sintered in air at temperatures from 900 °C to 1150 °C. $Bi_4Ti_3O_{12}$ samples with and without 5 wt.% templates were named as BIT-T and BIT-N in the following text, respectively.

2.3. Characterization

The densities of the sintered laminates were measured by the Archimedes method. Grain orientation was examined based on intensities of X-ray diffraction (XRD) peaks, and the Lotgering factor (*f*) was calculated as described in Ref. 13. The microstructures of the green and sintered laminates were observed by SEM (Hitachi S-570). Dielectric constants in directions parallel and perpendicular to the casting plane as a function of temperature were determined by an impedance analyzer (HP4192A) at frequencies of 100 KHz and 1 MHz, respectively.

3. Results and discussion

3.1. Template orientation during tape casting

Fig. 1(a) and (b) shows the SEM images of the surfaces parallel and perpendicular to the casting plane of a debindered BIT-T sample, respectively. The $Bi_4Ti_3O_{12}$

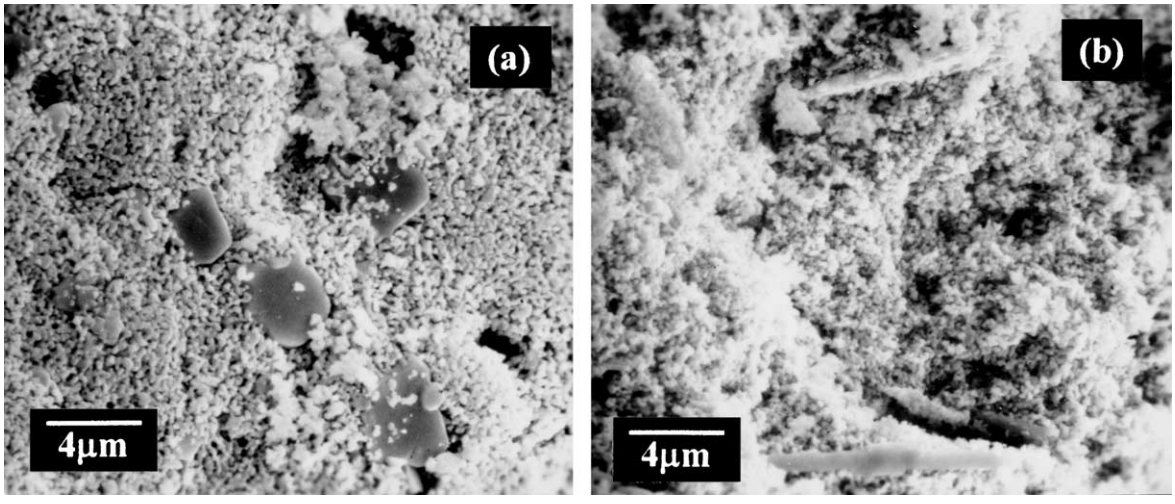

Fig. 1. SEM images of debindered Sample BIT-T: (a) surface parallel to the casting direction and (b) fracture surface perpendicular to the casting direction.

template particles are piled up along their *c*-axis in the matrix, with their major surface planes oriented in parallel to the casting plane. The alignment of the template particles is mainly due to the high aspect ratio of the $Bi_4Ti_3O_{12}$ platelets and the shearing force exerting on the particles during tape casting.[14] When the blade passes the slurry surface, the platelets tend to align under the influence of the shearing force, and the interaction between the platelets and the fine matrix particles makes the platelets align in the same orientation in the cast.[10]

3.2. Sintering

Fig. 2 shows the sintering behavior of the BIT-N sample and BIT-T sample. The BIT-N sample was rapidly densified between 900 °C and 950 °C, a maximum relative density of 97.5% was obtained at 1000 °C, and then the density declined slightly when the sintering temperature was increased to 1050 °C. In comparison with that of BIT-N sample, sintering of BIT-T sample proceeded more slowly. The maximum relative density for BIT-T sample, which was 97.0%, was achieved at 1100 °C, almost 100 °C higher than that of BIT-N. The poor sinterability of BIT-T is caused by the large $Bi_4Ti_3O_{12}$ platelet particles included in the matrix. These particles behave as rigid inclusions in the matrix, causing a tensile stress in their vicinity during sintering. This tensile sintering stress counteracts the sintering driving force, and decreases the sintering ability of the BIT-T sample. Furthermore, as stated in a later section (seeing Fig. 4), the addition of large template particles in its starting powder leads to a remarkable increase in the average grain size of the BIT-T sample, which is another factor for hindering the materials densification.

3.3. Grain orientation in the sample BIT-T

Fig. 3 shows the XRD patterns of sample BIT-T sintered under different conditions. Samples showed in Fig. 3(a)–(c) were sintered for the same soaking time and at the same heating rate but at different temperatures. It can be seen that with an increase in the sintering temperature, the diffractions from the (*00l*) planes of $Bi_4Ti_3O_{12}$ progressively dominate the XRD pattern. The Lotgering factor (*f*) calculated according to the XRD results showed a value of 0.32, 0.64 and 0.91 for the sample sintered at 1000 °C, 1100 °C and 1150 °C, respectively, indicating a more textured material with increasing sintering temperature. In addition to the sintering temperature, the development of grain orientation in the sample is also influenced by the soaking time [see Fig. 3(b) and (d)] and the heating rate [see Fig. 3(d) and (e)]. Under the same heating rate (150 °C/h), when the soaking time at 1100 °C is prolonged from 2 h to 4 h, the *f* value increases correspondingly from 0.64 to 0.85. On the other hand, keeping the soaking time (4 h) at 1100 °C constant and increasing the heating rate from 150 °C/h to 600 °C/h, the *f* value increases correspondingly from 0.85 to 0.92.

The development of high grain orientation in the BIT-T samples can be understood as follows. As well known,

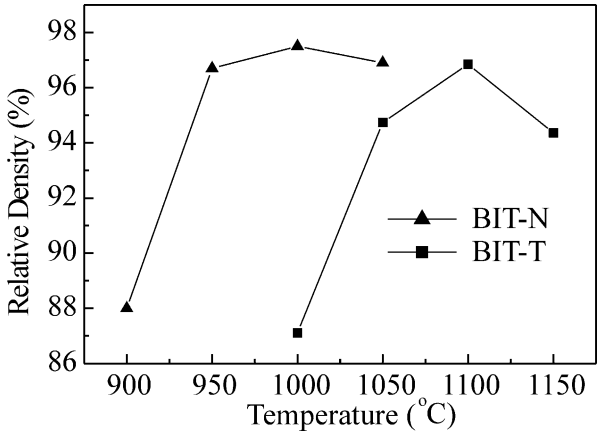

Fig. 2. Relative densities of sintered laminates without (BIT-N) and with 5 wt.% (BIT-T) platelets as a function of temperature.

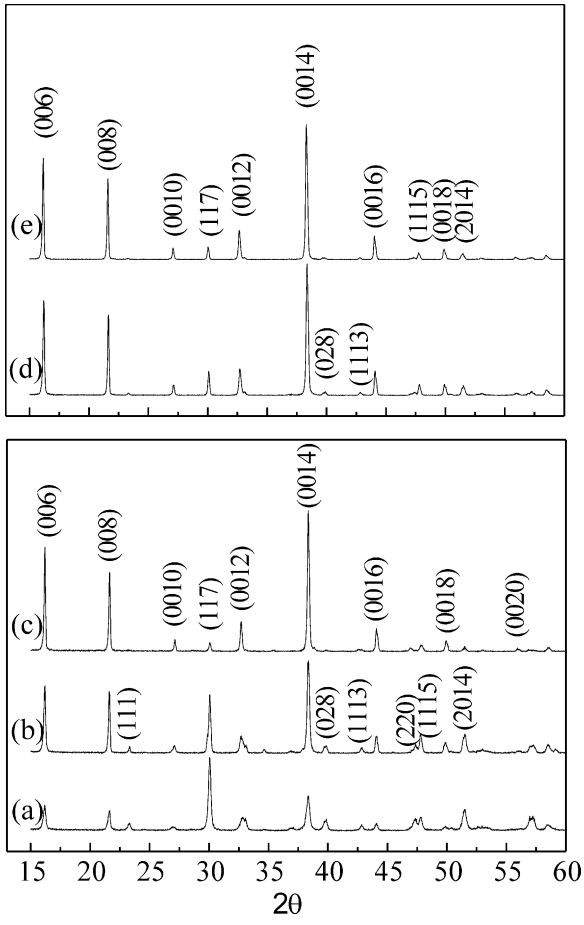

Fig. 3. X-ray diffraction patterns of BIT-T sintered at different conditions: (a) 1000 °C for 2 h, 150 °C/h heating; (b) 1100 °C for 2 h, 150 °C/h heating; (c) 1150 °C for 2 h, 150 °C/h heating; (d) 1100 °C for 4 h, 150 °C/h heating; and (e) 1100 °C for 4 h, 600 °C/h heating.

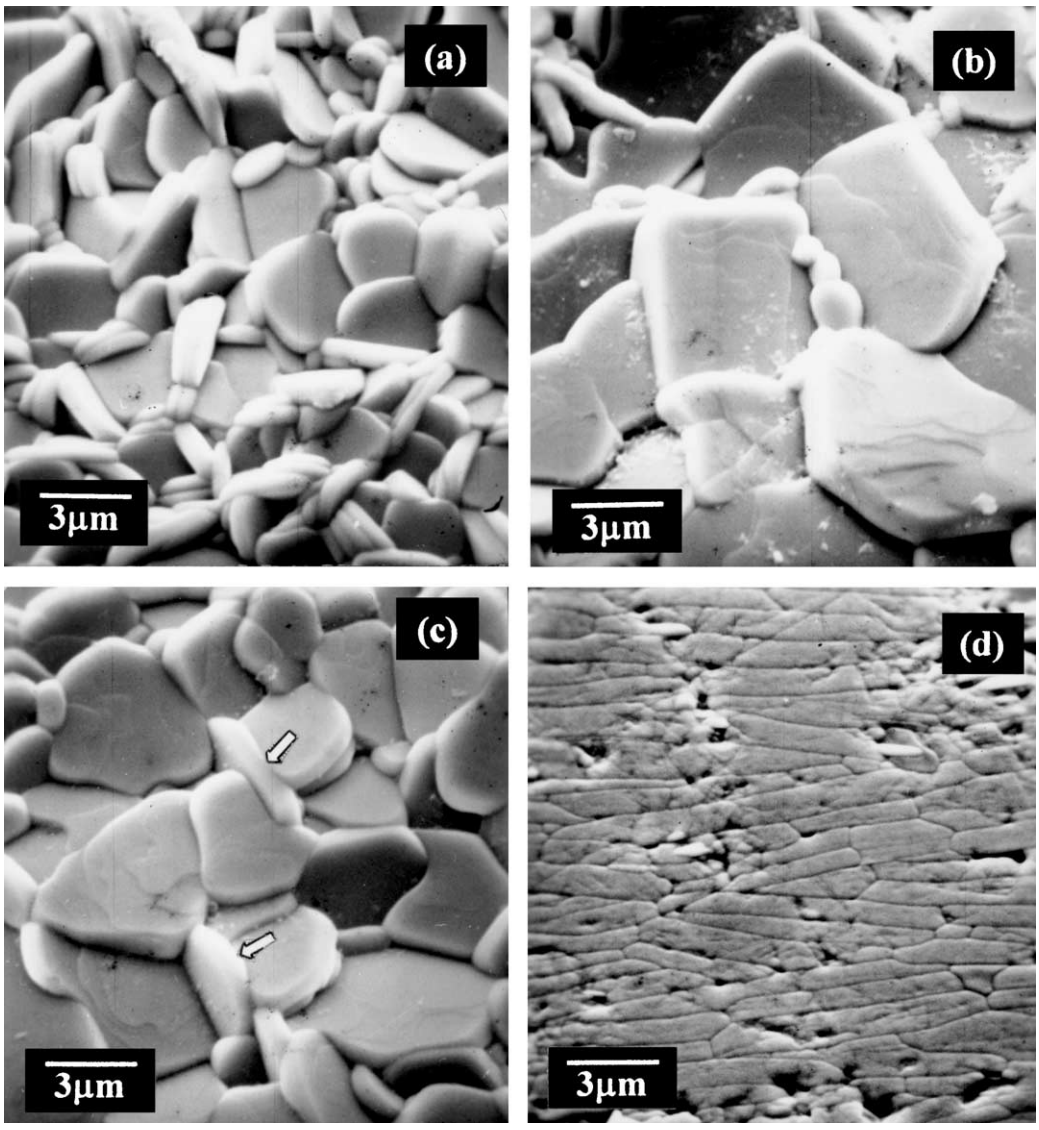

Fig. 4. SEM images of natural surface parallel to the tape casting direction: (a) BIT-N sintered at 1100 °C for 4 h at a heating rate of 600 °C/h; (b) BIT-T sintered at 1100 °C for 4 h at a heating rate of 600 °C/h; (c) BIT-T sintered at 1100 °C for 4 h at a heating rate of 150 °C/h and (d) polished and etched surface perpendicular to the casting direction of BIT-T sintered at 1150 °C for 4 h at a heating rate of 300 °C/h.

the grain boundary has a higher internal energy than the inside of grains. In order to reduce the grain boundary area and thus the internal energy of the system, the small matrix grains tend to be consumed by the large templates via an Ostwald ripening process during sintering, because of the grain size and the "specific grain boundary area" differences between the matrix and the template grains. However, due to the anisotropy of the $Bi_4Ti_3O_{12}$ grain boundary energy, the consumption of the matrix grains by the template grains shows a high selectivity, as explained below.

The (*00l*) planes of $Bi_4Ti_3O_{12}$ crystal possess low surface energy and tends to develop more fully during sintering.[10] As a result, almost all of the $Bi_4Ti_3O_{12}$ grains develop into a plate-like morphology at the early stage of sintering, with their main surface planes parallel to the (*00l*) crystal planes. The plate-like matrix grains oriented parallel to the templates form low-energy grain boundaries with the templates, and are difficult to be consumed. Some of them can grow large and eventually remain in the final product. In contrast, the matrix grains misaligned in a large angle with the templates form high-energy grain boundaries with the templates and are readily consumed not only by the templates but also by the matrix grains that oriented in parallel to the templates. As a result, the volume fraction of the randomly oriented grains in the sample is reduced, and concurrently the degree of grain orientation increases with sintering temperature and time.

The degree of grain orientation is also affected by the heating rate because it controls the growth rate of fine matrix grains during the heating process. When the heating rate is low, the fine matrix particles have more chance to grow during heating, leading to the formation

of coarser matrix grains in the sample. The formation of larger matrix grains reduced the grain size difference between the matrix and the template grains, and decreased the driving force for Ostwald ripening of the templates to consume the small matrix grains in the later stage of sintering. When some matrix grains become too large to be consumed by the templates, they are misaligned with respect to the templates and impinge upon the well-aligned grains [see Fig. 4(c)], leading to lower degree of orientation. While at a higher heating rate, the matrix largely consists of fine grains even at the final sintering stage, and thus most of them will be consumed through Ostwald ripening by the templates, resulting in higher degree of grain orientation in the sintered sample.

3.4. Microstructure

Fig. 4(a) and (b) show the SEM micrographs of the natural surfaces (parallel to the tape casting direction) of BIT-N and BIT-T samples sintered at 1100 °C for 4 h under a heating rate of 600 °C/h. The grain orientation in BIT-N [Fig. 4(a)] is completely random ($f = 0.28$) and the grain size is small. However, as 5 wt.% template particles are added (BIT-T), both the grain size and the orderliness of grain orientation in the sample are significantly increased [Fig. 4(b), $f = 0.92$]. In this sample, the large plate-like grains orient in parallel to the tape-casting direction with some tiny grains located at their triple junctions. The much larger grain size in the BIT-T sample than that in the BIT-N sample unambiguously testifies an Ostwald ripening process in which the templates consume the fine matrix grains during sintering. The tiny grains in the BIT-T sample are the residual matrix grains that have not been completely consumed by the template grains during sintering.

Fig. 4(c) shows the SEM micrograph of the natural surface (parallel to the tape casting direction) of a BIT-T sample sintered at 1100 °C for 4 h under a low heating rate of 150 °C/h. It can be seen that this sample also shows a high order of grain orientation ($f = 0.85$). Its grain size is smaller than that of the BIT-T sample showed in Fig. 4(b), but larger than that of the BIT-N sample showed in Fig. 4(a). In addition to many tiny grains, some misoriented large grains (indicated by arrows) are also found in this sample as well [Fig. 4(c)].

The microstructure difference between the two BIT-T samples shown in Fig. 4(b) and (c) shows the effect of heating rate on the microstructure development. Due to the slow heating rate in sintering, the matrix grains in the BIT-T sample grow large and become difficult to be consumed by the template grain growth. As a result, the template grains undergo a relatively slower grain growth, which leads to the formation of relatively smaller grains in the sintered sample [Fig. 4(c)] comparing to BIT-T sample shown in Fig. 4(b).

Fig. 4(d) shows the SEM image of the polished surface perpendicular to the casting direction of the BIT-T sample sintered at 1150 °C for 4 h. From this picture, the highly textured structure can be clearly seen. The plate-like $Bi_4Ti_3O_{12}$ grains are aligned in a high order along their length direction and are about 6-10 μm in length and 1 μm in thickness.

3.5. Electrical properties

The dielectric constants of a BIT-T sample sintered at 1100 °C in the directions parallel and perpendicular to the tape-casting plane are measured as a function of temperature at 100 KHz [Fig. 5(a)] and 1 MHz [Fig. 5(c)], respectively. The dielectric data show a high anisotropy, as observed by Takenaka, Swartz and Sech in the other textured BIT ceramics.[1,15,16] In the present work, the exact values of room temperature dielectric constant are 160 and 130 for the directions parallel and perpendicular to the casting plane at both frequencies, which agree well with the single-crystal values and those obtained by previous workers in textured BIT.[1,15–17] When the temperature increases beyond 200 °C, the dielectric constants in both directions increase rapidly; at the same time, the dielectric constant difference between the two directions became increasingly large. The dielectric constant in the direction parallel to the casting plane are three times larger than that in the direction perpendicular to the casting plane at 450 °C and 100 KHz, and two times larger at 450 °C and 1 MHz, as shown in Fig. 5.

In addition, by comparing Fig. 5(a) with (c), it is found that the dielectric constants in both directions show a significant decrease as the frequency is increased from 100 KHz to 1 MHz, due to the suppression of space charge polarization and dielectric relaxations at higher frequency. And this decrease in dielectric constant is especially remarkable in the direction parallel to the casting plane, because of the higher conductivity and the more significant contributions of space charge polarization and dielectric relaxations to dielectric constant in this direction.

Fig. 5(b) and (d) show the dielectric loss of BIT-T in the directions parallel and perpendicular to the tape-casting plane. As expected, the dielectric loss also shows a great anisotropy, with the dielectric loss in the direction parallel to casting plane showing a much larger value. Fig. 5(b) clearly shows a hump in the loss tangent at 100 KHz, corresponding to the onset of the dielectric relaxations and space charge polarization contribution to the dielectric constant. This effect is more evident in the direction parallel to the casting plane than in the direction perpendicular to the casting plane. Such an anisotropy in the loss tangent is reasonable from the viewpoint that the conductivity along the *a–b* plane (i.e. the direction parallel to the casting plane) is much

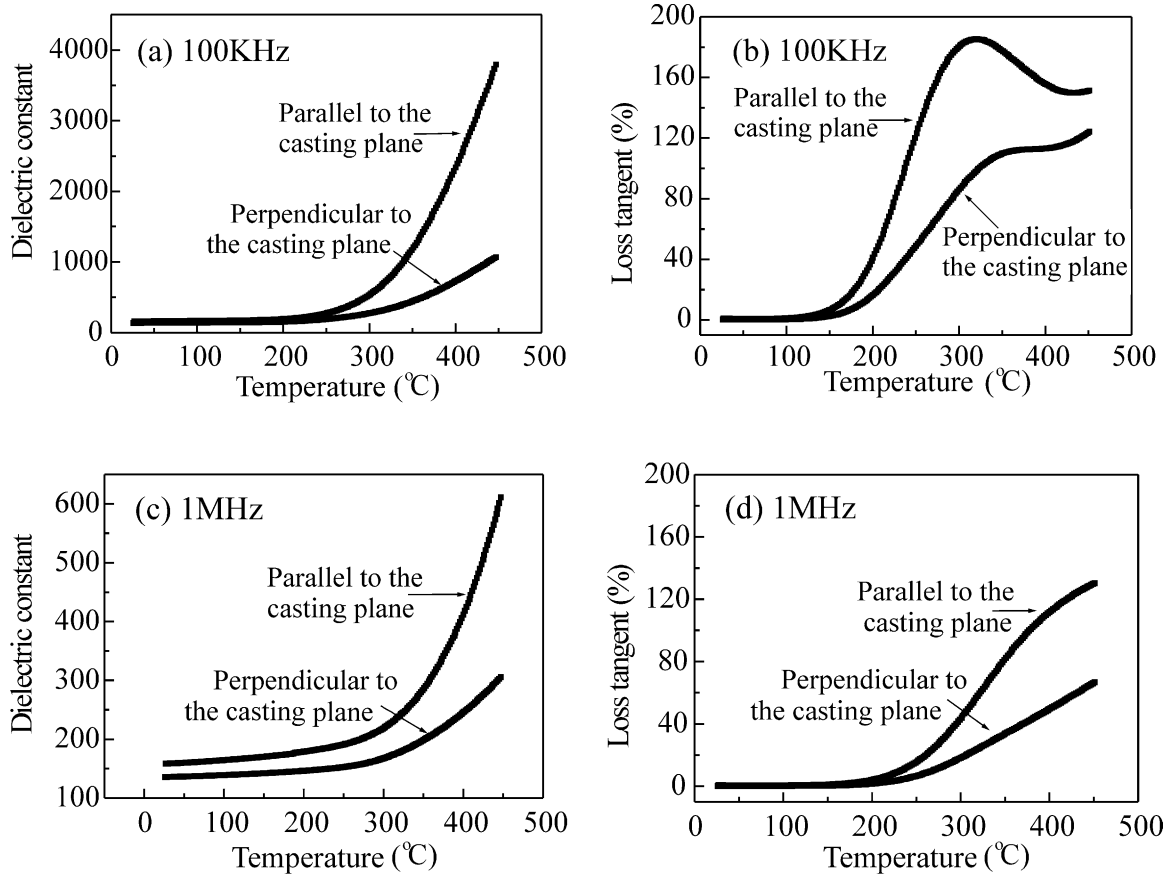

Fig. 5. Dielectric constants (a, c) and loss tangents (b, d) of BIT-T sintered at 1100 °C for 4 h in directions parallel and perpendicular to the tape-casting plane.

higher relative to the *c*-direction (i.e. the direction perpendicular to the casting plane).[18] The room temperature values of loss tangent at 100 KHz and 1 MHz are 0.01 and 0.006 for the directions parallel to the casting plane, and are 0.002 and 0.001 for the direction perpendicular to the casting plane, respectively.

4. Conclusions

1. The large $Bi_4Ti_3O_{12}$ template particles strongly retarded the sintering of BIT-T sample, and under the same sintering conditions, the $Bi_4Ti_3O_{12}$ sample containing templates showed a much larger grain size and a higher degree of grain orientation than the $Bi_4Ti_3O_{12}$ sample without the templates.
2. The selective consumption of the matrix grains by the orderly aligned template grains in the Ostwald ripening process was mainly responsible for the high degree of grain orientation in the BIT-T sample.
3. The degree of grain orientation in the BIT-T sample increased with the increase in sintering temperature, soaking time and heating rate.
4. The BIT-T sample showed anisotropic dielectric properties in the directions parallel and perpendicular to the casting plane, due to the formation of highly textured microstructure in it. This anisotropy became more significant at temperatures close to the material's Curie temperature.

Acknowledgements

This work was supported by National Natural Sciences Foundation of China and The Outstanding Overseas Chinese Scholars Fund of Chinese Academy of Sciences.

References

1. Takenaka, T. and Sakata, K., Grain orientation and electrical properties of hot-forged $Bi_4Ti_3O_{12}$. *Jpn. J. Appl. Phys.*, 1980, **19**, 31–39.
2. Hirao, K., Ohashi, M., Brito, M. E. and Kanzaki, S., Processing strategy for producing highly anisotropic silicon nitride. *J. Am. Ceram. Soc*, 1995, **78**, 1687–1690.
3. Youngblood, G. E. and Gordon, R. S., Textured-conductivity

relationship in polycrystalline lithia-stabilized β″-alumina. *Ceram. Internal.*, 1978, **4**, 93–98.
4. Ma, Y. C. and Bowman, K. J., Texture in hot-pressed or hot-forged alumina. *J. Am. Ceram. Soc.*, 1991, **74**, 2941–2944.
5. Inoue, Y., Kimura, T. and Yamaguchi, T., Grain orientation and electrical properties of hot-pressed bismuth titanate ceramics. *Yogyo-Kyokai-Shi*, 1984, **92**, 54–57.
6. Igarashi, H., Matsunaga, K., Taniai, T. and Okazaki, K., Dielectric and piezoelectric properties of grain-oriented $PbBi_2Nb_2O_9$ ceramics. *Am. Ceram. Soc. Bull.*, 1978, **57**, 815–817.
7. Seabaugh, M. M., Kerscht, I. H. and Messing, G. L., Texture development by templated grain growth in liquid-phase-sintered α-alumina. *J. Am. Ceram. Soc.*, 1997, **80**, 1181–1188.
8. Sacks, M. D., Scheiffele, G. W. and Staab, G. A., *J. Am. Ceram. Soc.*, 1996, **79**, 1611–1616.
9. Duran, C., T-Mckinstry, S. and Messing, G. L., Fabrication and electrical properties of textured $Sr_{0.53}Ba_{0.47}Nb_2O_6$ ceramics by templated grain growth. *J. Am. Ceram. Soc.*, 2000, **83**, 2203–2212.
10. Horn, J. A., Zhang, S. C., Messing, G. L. and T-Mckinstry, S., Templated grain growth of textured bismuth titanate. *Am. Ceram. Soc.*, 1999, **82**, 921–926.
11. Dorrian, J. F., Newnham, R. E. and Smith, D. K., Crystal structure of $Bi_4Ti_3O_{12}$. *Ferroelectrics*, 1971, **3**, 17–27.
12. Kan, Y. M., Wang, P. L., Li, Y. X., Cheng, Y. B. and Yan, D. S., Nano-sized $Bi_4Ti_3O_{12}$ powder prepared by the hydrolysis process. *Key Engineering Materials*, 2002, **224-226**, 597–600.
13. Lotgering, K., Topotactical reactions with ferromagnetic oxides having hexagonal crystal structureds-I. *J. Inorg. Nucl. Chem.*, 1959, **9**, 113–123.
14. Chazono, H., Kimura, T. and Yamaguchi, T., Fabrication of grain-oriented $Bi_4Ti_3O_{12}$ ceramics by normal sintering—I. Tape-casting and sintering. *Yogyo-Kyokai-Shi*, 1985, **93**, 485–490.
15. Swarz, S., Schulze, W. A. and Biggers, J. A., Fabrication and electrical properties of grain oriented $Bi_4Ti_3O_{12}$ ceramics. *Ferroelectrics*, 1981, **38**, 765–768.
16. Sech, V. K. and Schulze, W. A., Grain-oriented fabrication of bismuth titanate ceramics and its electrical properties. *IEEE Transaction on Ultrasonics, Ferroelectrics, and Frequency Control*, 1989, **36**, 41–49.
17. Fouskova, A. and Cross, L. E., Dielectric properties of bismuth titanate. *J. Appl. Phys.*, 1970, **9**, 113–123.
18. Kim, S. K., Miyayama, M. and Yanagida, H., Electrical anisotropy and a plausible explanation for dielectric anomaly of $Bi_4Ti_3O_{12}$ single crystal. *Mater. Res. Bull.*, 1996, **31**, 121–131.